An accurate RSS/AoA-based localization method for internet of underwater things

Azadeh Pourkabirian [a], Fereshteh Kooshki [b], Mohammad Hossein Anisi [c],[*], Anish Jindal [d]

[a] Department of Computer and Information Technology Engineering, Qazvin Branch, Islamic Azad University, CO, Qazvin 34199-15195, Iran
[b] Department of Mathematics, Qazvin Branch, Islamic Azad University, CO, Qazvin 34199-15195, Iran
[c] School of Computer Science and Electronic Engineering, University of Essex, Colchester CO4 3SQ, United Kingdom
[d] Department of Computer Science, Durham University, Durham DH1 3LE, United Kingdom

ABSTRACT

Localization is an important issue for Internet of Underwater Things (IoUT) since the performance of a large number of underwater applications highly relies on the position information of underwater sensors. In this paper, we propose a hybrid localization approach based on angle-of-arrival (AoA) and received signal strength (RSS) for IoUT. We consider a smart fishing scenario in which using the proposed approach fishers can find fishes' locations effectively. The proposed method collects the RSS observation and estimates the AoA based on error variance. To have a more realistic deployment, we assume that the perfect noise information is not available. Thus, a minimax approach is provided in order to optimize the worst-case performance and enhance the estimation accuracy under the unknown parameters. Furthermore, we analyze the mismatch of the proposed estimator using mean-square error (MSE). We then develop semidefinite programming (SDP) based method which relaxes the non-convex constraints into the convex constraints to solve the localization problem in an efficient way. Finally, the Cramer–Rao lower bounds (CRLBs) are derived to bound the performance of the RSS-based estimator. In comparison with other localization schemes, the proposed method increases localization accuracy by more than 13%. Our method can localize 96% of sensor nodes with less than 5% positioning error when there exist 25% anchors.

1. Introduction

Recently, the fourth industrial revolution known as the Industrial Internet of Things (IIoT) [1] has emerged to improve industrial productivity and manufacturing. An extension of IIoT is in the underwater environment, namely, the Internet of Underwater Things (IoUT) that connects smart underwater objects for ocean exploration. IoUT comprises a large number of smart connected devices such as sensors and actuators that are distributed in a specific aquatic environment to execute collaborative monitoring and data collection tasks. IoUT is used in a wide range of applications [2–4], e.g., environmental monitoring, deep sea archaeology, smart fishing, etc.

Fisheries throughout the world are in danger of collapsing. There's not too much fish in our diet - there's just too much wasteful and shortsighted fishing in the last few decades. Many species are in danger of extinction due to overfishing. In unselective fishing, fishermen catch millions of fish unwillingly and the dead or dying bycatch is usually thrown back into the ocean. Nevertheless, various fishermen and communities all over the world depend on fishing for food or income. IoUT has great potential to develop effective fishing approaches. Smart sensors of IoUT can be used to detect the type of fish and prevent catching endangered aquatic species. Furthermore, they can help to find the fish stocks in the ocean. IoUT connects the ocean's bottom to the water surface through multi-hop paths. With the knowledge of fish locations, fishers can catch fish more effectively. However, due to the harsh environments in oceans and the dynamic characteristics of underwater transmission channels, these networks face several technical challenges [5] including acoustic communication, energy efficiency, mobility, reliability, and etc. In addition, underwater applications such as smart fishing require the location information of sensor nodes for tracking fish. Therefore, localization is a critical issue in IoUT.

In this paper, we aim to develop an autonomous system for smart fishing using smart IoUT objects.

The main contributions of this work are summarized as follows:

* Corresponding author.
    E-mail address: m.anisi@essex.ac.uk (M.H. Anisi).

- We propose an accurate hybrid AoA/RSS localization approach for the smart fishing use case. The proposed method aims to localize underwater sensors for monitoring underwater environment under noisy distance information. Since smart sensors can detect the type and the position of fish, our method avoids catching endangered fish and help fishermen to find fish stock.
- The proposed method estimates the position of sensors when perfect information about the background noise is not available. To solve the localization problem in the polynomial time, we convert the non-convex constraints into the convex constraints and then transform the localization problem into an SDP problem. We derive MSE of the proposed estimator to measure the estimation error under fading acoustic communications.
- Furthermore, to optimize the worst-case performance, a minimax method is developed that minimizes the maximum location estimation error. Finally, the CRLB as a benchmark is derived to determine a lower bound on the MSE of the proposed estimator to bound the performance of the proposed approach over the measuring error.
- The computational complexities of the proposed method are investigated and compared to two other related schemes. Simulation results verify the correctness of our theoretical analysis and show that the proposed method effectively improves the location accuracy.

The rest of the paper is structured as follows: Section 3 presents the system description and assumptions of the problem. In Section 4, we define the proposed AoA/RSS-based localization approach and then formulate the problem as a semidefinite programming. Section 5 provides the performance evaluation of the proposed method. We present the computational complexity of our scheme and derive the Fisher information matrix (FIM) and CRLB to evaluate the performance of the proposed estimator. Numerical results of the proposed model are discussed in Section 6 for validation purposes. Finally, we draw conclusions in Section 7.

2. Related works

In recent years, numerous localization methods [6–8] have been proposed in the literature. Fig. 1 illustrates the classification of underwater localization schemes. Generally, the existing localization methods is divided into two main categories: distributed approaches and centralized methods. Although the distributed schemes are more scalable, they often suffer from error propagation and converge slower to the optimal solution.
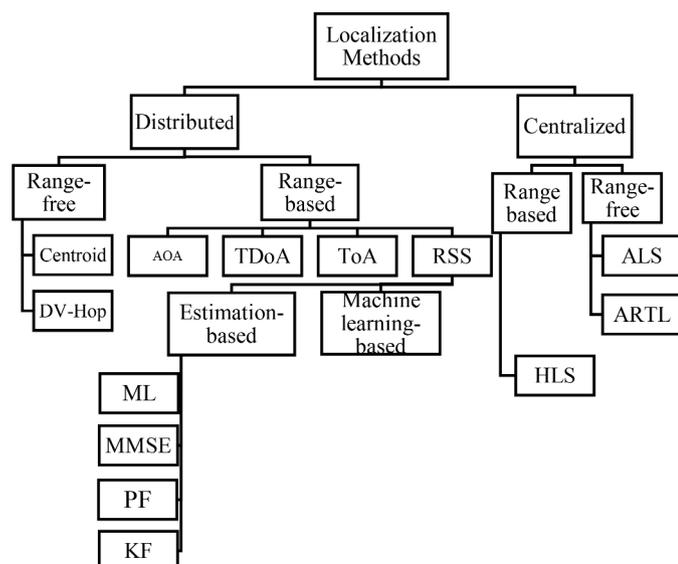

Fig. 1. Underwater localization techniques.

In contrast, the centralized methods have lower scalability however they are more accurate in positioning since they have access to all location's information in the network. Some distributed studies were investigated in [9,10] for large-scale IoUT. However, because of high transmission loss and underwater acoustic noise, these methods often cannot work well in harsh aquatic environments. The authors in [11] provided a review on game-theoretic localization methods in underwater sensor networks. They studied the sensors cooperation and coordination via game theory framework. Moreover, they compared several game-based localization schemes under different metrics.

On the other hand, the localization methods can be classified based on the factors [12–16] used for position estimation including received signal strength (RSS), time-difference-of-arrival-based (TDoA), time-of-arrival-based (ToA), round-trip-time-based (RTT-based), or angle-of-arrival-based (AoA). In [17–23], the authors proposed localization schemes with ToA or AoA assistance for large-scale underwater sensor networks. Table 1 provides a classification of underwater localization schemes. The studies [24,25] presented frameworks for simultaneously synchronizing and localizing to provide more localization accuracy. They modeled stratification effect of underwater medium using the ray-tracing method. An algorithm was presented in [26] that calculates the Doppler shift and Doppler differentials between all sensor pairs.

Although, localization based on TDoA, ToA, or RTT measurements gives more accurate estimation results, these techniques need exact clock synchronization and timing. RSS-based localizations methods have less accuracy comparing to other localization schemes such as ToA-based methods due to the line-of-sight assumption which is impractical for multi-path underwater communication environments. However, they have less complexity for implementation and do not require any specialized hardware. On the other hand, AoA-based measurements successfully decrease the effect of measurement noises and remarkably improve the localization accuracy as it involves multi-path components in the localization process and relaxes the line-of-sight assumption. In this paper, we propose a hybrid localization method to take advantage from simplicity and accuracy of AoA and RSS methods at the same time.

Many localization algorithms based on the RSS and AoA measurements [27–33] have been proposed for underwater wireless sensor networks. The authors in [27] proposed a three-dimensional AoA-based algorithm to localize multiple mobile sensors. They claimed that the proposed method has small operational latency. In [28], the authors developed an energy-efficient localization scheme based on RSS measurements in optical underwater sensor networks where range estimation is challenging due to seawater channel impairments and optical noise sources. The authors in [29–33] addressed the target localization problem using RSS measurements in acoustic communications where the target transmit powers are examined in different cases. In [34], the positioning problem considering transmission loss (TL) phenomena were investigated. The problem was modeled as the Lambert W function and compared to Newton-Raphson inversion. In [35,36], robust localization methods were presented using range measurements that bounds estimation error. The authors translated the nonconvex optimization problem to a convex problem and solved the problem using SDP. A target localization method based on a hybrid AoA and RSS measurements for the acoustic network in the underwater environment was proposed in which the transmit power of the target node is considered an unknown parameter [37]. The authors in [38] designed a localization scheme for tracing a scuba diver without GPS equipment in the underwater environment. The divers send SOS messages using underwater acoustic communication. The algorithm has high computational complexity, which might restrict its application in large-scale underwater wireless sensor networks. In [39], the acoustic localization problem was studied using the decision tree method. the authors developed a signal selection algorithm considering the amplitude, ToA, bandwidth, and Doppler frequency of the detected pulses as the input features. A novel acoustic system that combined inaudible sensing and

Table 1
Underwater localization classification.

Method	Range based/Range free	Ranging method	Sync	Localization Coverage	Computational Complexity	Estimation accuracy	Energy efficient
Cluster-based localization [12]	Range based	TDoA	Yes	High	High	High	Yes
AoA/ToA localization [13]	Range based	AoA/ToA	Yes	Low	High	High	Not specified
Bayesian localization [14]	Range free	–	No	Not specified	Low	High	Yes
Energy-efficient localization [18]	Range free	–	Yes	Not specified	High	Low	Yes
AoA localization [19]	Range based	AoA	Yes	High	High	High	Not specified
Secure range-based localization [20]	Range based	ToA	Yes	Not specified	High	Not specified	Not specified
RSS-based localization [21]	Range based	ToF/RSS	Yes	Not specified	High	High	Not specified
Semi-blind localization [23]	Range based	LOS	Yes	Low	Low	High	Yes
Silent localization [24]	Range based	RSSI	Yes	Not specified	Not specified	High	Not specified
Energy Harvesting localization [28]	Range based	RSS	Yes	Low	Not specified	High	Yes

communication in an inaudible band (18–22 kHz) was designed in [40]. The work of [41] proposed a cooperative localization scheme for autonomous underwater vehicles. They used the adaptive neuro-fuzzy inference system to overcome the effect of abnormal acoustic ranging errors. The authors in [42] developed a Q-learning-based data collection and path planning method for autonomous underwater vehicle (AUV) that reduces energy consumption and latency. The study [43] proposed an energy-based localization algorithm based on RSS difference (RSSD) model. The authors defined a Cramér-Rao lower bound as a performance benchmark to measure MSE of location estimation. In [44], a location prediction algorithm based on Doppler shift estimation was presented for underwater acoustic sensor networks that enhances the estimation accuracy. Study [45] developed a hybrid DDS/TDOA method for underwater localization which is robust to imperfect node clocks.

3. System description

We consider an IoUT network consisting of different types of smart objects including a BS, *N* sensor nodes, *M* anchor nodes, wireless cameras, and smartphones. The BS which has more capabilities in storage and computational performs the data analysis. Smart sensors with different measurement capabilities collect data about the angle, temperature, ocean tension, distance, and depth from the ocean's bottom and send their observations to the BS on the water surface. On the other hand, fishing nets are equipped with microcontrollers that control and automate them. The sensing measurements are remotely accessible from every internet connected IoT device. Thus, fishers are able to connect to the fishing environment and monitor the ongoing conditions from anywhere and anytime. Fig. 2 shows an example of smart fishing design and deployment.

In the proposed scenario, anchor nodes with known locations $a_i = [a_{ix} a_{iy}]$ are randomly deployed and equipped with omnidirectional antennas. We consider a disk-based sensing model with a sensing radius *r* for each smart node. Wireless smart sensors are uniformly and independently distributed. We assume that the anchor nodes determine their positions using GPS modules and nodes, with unknown location information $s_j = [s_{jx} s_{jy}]$, obtain their location based on the AoA/RSS measurements from anchor nodes (Fig. 3).

4. AoA/RSS-based localization

According to the acoustic transmission loss model, the RSS measurement between the anchor node *j* and sensor node *i* can be defined as [28]:

$$P_j^{re} = P_i^{tr} \rho \Gamma_{ij} \frac{R_j \cos\theta_2}{2\pi d_{ij}^2(1 - \cos\theta_1)} \tag{1}$$

where P_j^{re} denotes the received power at the sensor node *j*, P_i^{tr} is the
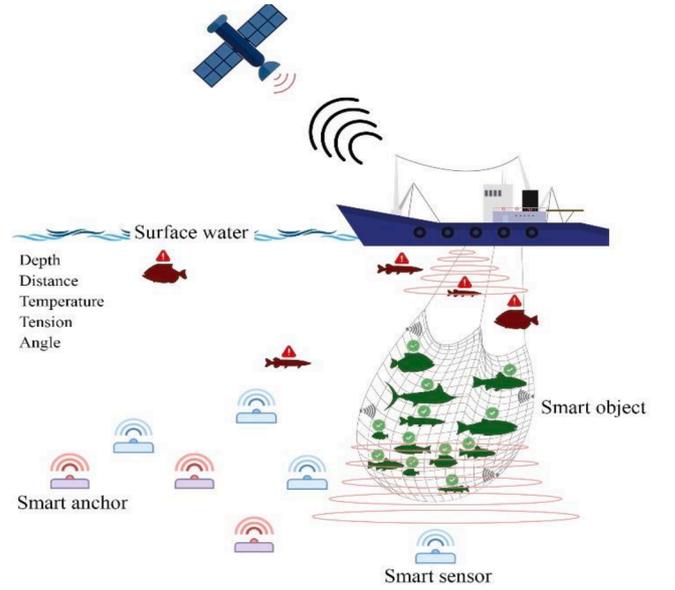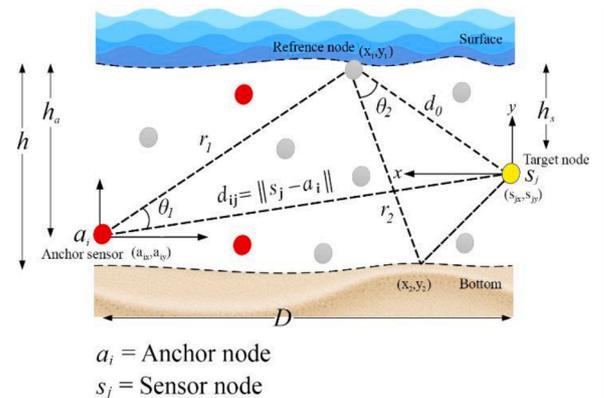

Fig. 2. Smart fishing scenario.

Fig. 3. Positions of underwater nodes.

transmit power at the anchor node *i*, ρ indicates water's electrical conductivity, $\Gamma_{ij} = exp^{-\gamma d_{ij}}$ represents the propagation loss in which γ denotes the path loss coefficient, and $d_{ij} = \|s_j - a_i\|$ identifies the distance between the sensor node *j* and the anchor node *i*, R_j states the coverage area of node *j*, θ_2 determines AoA at the receiver node, and θ_1 is the departure angle of the transmitted signal *D* states horizontal distance between the source node and the target node, h_a denotes the depth of the

anchor node, and h_s is the depth of the sensor node from the sea surface. In order to calculate the distance from RSS measurements (Fig. 3), we need a transfer function as follows:

$$d_{ij} \overset{\Delta}{=} f\left(P_j^{re}\right) = \frac{2}{\gamma} \Re_0 \left(\frac{\gamma}{2} \sqrt{\frac{P_i^{tr} \rho R_j \cos\theta_2}{P_j^{re} 2\pi(1 - \cos\theta_1)}}\right) \tag{2}$$

where $\Re_0(\cdot)$ denotes the real part of Lambert-W function.

Although the RSS measurement in (1) merely considers propagation loss and scattering, the distance measurement in (2) is erroneous and makes localization inaccurate because of propagation channel effects. Thus, we use AoA measurements to improve the accuracy of location estimation through evaluating more accurate channel characteristics. The workflow of the proposed method is described in Fig. 4.

The probability density function (PDF) of AoA for a signal along sea surface and bottom in an acoustic channel can be evaluated as:

$$f_{\theta_1}(\theta_1) = \int_0^{R_1} \int_{\theta_2 = -\pi/2}^{-\tan^{-1}\left(\frac{h_a}{D - r_1 \cos\theta_1}\right)} \int_{-\left(\frac{h_a}{\sin\theta_2}\right)}^{R_2} f(r_1, \theta_1, r_2, \theta_2) \, dr_2 d\theta_2 dr_1 \tag{3}$$

Where $R_1 = [(\cos\theta_1/D)^l + (\sin\theta_1/h_a)^l]^{-1/l}$ and $R_2 = [(\cos\theta_2/(D - r_1\cos\theta_1))^l + (\sin\theta_2/h)^l]^{-1/l}$ identify scattering regions for the signals from surface and bottom, respectively so that $0 \leq r_i \leq R_i, \forall i$, $l \gg 2$ is an even value to make sure that d_i is within the range specified and a rectangular region of θ_i is covered. In polar coordinates, the joint PDF $f(r_1, \theta_1, r_2, \theta_2)$ corresponds to:

$$f(r_1, \theta_1, r_2, \theta_2) = \prod_{b=1}^{n_b} \prod_{s=2}^{n_s} r_1 r_{2b} r_{2s-1} f\left(x_1, y_1, \ldots, x_{n_b}, y_{n_b}, x_{n_s}, y_{n_s}\right) \tag{4}$$

where n_b and n_s denote the number of scattered signals, r_b and r_s represent scattering regions for the signals, θ_b and θ_s are AoA at the

Fig. 4. Workflow of the proposed approach.

sensor node from the bottom and sea surface, respectively. Therefore, we can calculate the joint PDF of scattered location as below:

$$f\left(x_1, y_1, \ldots, x_{n_b}, y_{n_b}, x_{n_s}, y_{n_s}\right) = \frac{C \lambda_s^{n_s} \lambda_b^{n_b}}{D} e^{-\lambda_s(h_a - y_1)} \prod_{b=1}^{n_b} \prod_{s=2}^{n_s} e^{-\lambda_s(h_a - y_{2s-1}) - \lambda_b((h - h_a) + y_{2b})}$$
$$\times (1 - e^{-\omega_{2s-1} x_{2s-1}})(1 - e^{-\omega_{2b} x_{2b}}) \tag{5}$$

in which C is the normalization multiplier for a scattered signal from the bottom or surface, λ_s and λ_b identify the normalization multipliers for the surface uniform depth exponential distribution, ω_b and ω_s state the rate of change along the bottom or surface, $x_{2s-1} = \sum_{k=1}^{2s-1} r_k \cos\theta_k$, $x_{2b} = \sum_{k=1}^{2b} r_k \cos\theta_k$, $y_1 = r_1 \sin\theta_1$, $y_{2b} = r_{2b} \sin\theta_{2b} + h$, $y_{2s-1} = r_{2s-1} \sin\theta_{2s-1} - (h - h_a)$. Moreover, the estimated distance is expressed as:

$$\widehat{d}_{ij} = d_{ij} + e_{ij} \tag{6}$$

where e_{ij} states the estimation error. Moreover, each sensor can also use its previously known location information to estimate its current position as follows:

$$\widehat{s}_j(t) = s_j(t-1) - \left(\mathbb{D}^T \mathbb{D} + \delta I\right)^{-1} \mathbb{D}\left(\widehat{d}_{ij} - \Delta\left(\widehat{s}_j(t-1)\right)\right) \tag{7}$$

where δ denotes the step size, I stands for the identity matrix, $\Delta(\widehat{s}_j)$ identifies the error function and $\mathbb{D}$ states the distance matrix that is given by:

$$\mathbb{D} = \begin{bmatrix} 0 & \cdots & \widehat{d}_{1n}^2 \\ \vdots & \ddots & \vdots \\ \widehat{d}_{n1}^2 & \cdots & 0 \end{bmatrix}, \forall i \neq j \text{ and } \widehat{d}_{ij} > 0 \tag{8}$$

Now, we define the error function between the real Euclidean distance and the estimated distance as below:

$$\Delta(\widehat{s}_j) = \sum_{i=1}^N \left(\widehat{d}_{ij} \sqrt{(s_{jx} - a_{ix})^2 + (s_{jy} - a_{iy})^2}\right)^2 \tag{9}$$

Theorem 1. The minimum value of the error function $\Delta(\widehat{s}_j)$ which gives us the most accurate location estimation, is obtained at $(s_{1j}^*, s_{2j}^*, \ldots, s_{Nj}^*)$ so that

$$s_{jk}^* = \frac{\sum_{j=1}^M A_{kj} \widehat{d}_{ij}(d_{ij} + \widehat{d}_{ij})}{\sum_{j=1}^M \widehat{d}_{ij}(d_{ij} + \widehat{d}_{ij})}, r = 1, \ldots, N \tag{10}$$

in which r denotes a reference node.

Proof. See Appendix A. ∎

Proposition 1. The localization problem can be formulated as:

$$\min_{s_j, d_{ij}, z_j} z_j$$

s.t. $-z_j < \alpha_j d_{ij}^2 + \beta_j d_{ij} - 1 < z_j$

$$d_{ij}^2 = \| s_j - a_i \|_2^2 \tag{11}$$

and the optimization problem converges to the global solution when $e_{ij} = \alpha_j d_{ij}^2 + \beta_j d_{ij} - 1$.

Proof. See Appendix B. ∎

The main objective is to find $\widehat{s}$ that minimizes the size of the estimation error for all sensor nodes. To measure the location estimation quality, we use MSE criterion as follows:

$$MSE = \sum_{j=1}^N MSE_j \overset{\Delta}{=} E\{ \| \widehat{s}_j - s_j \text{AptCommand2016};^2 \}$$
$$= \left\{ (\widehat{s}_j - s_j)(\widehat{s}_j - s_j)^T \right\} \tag{12}$$
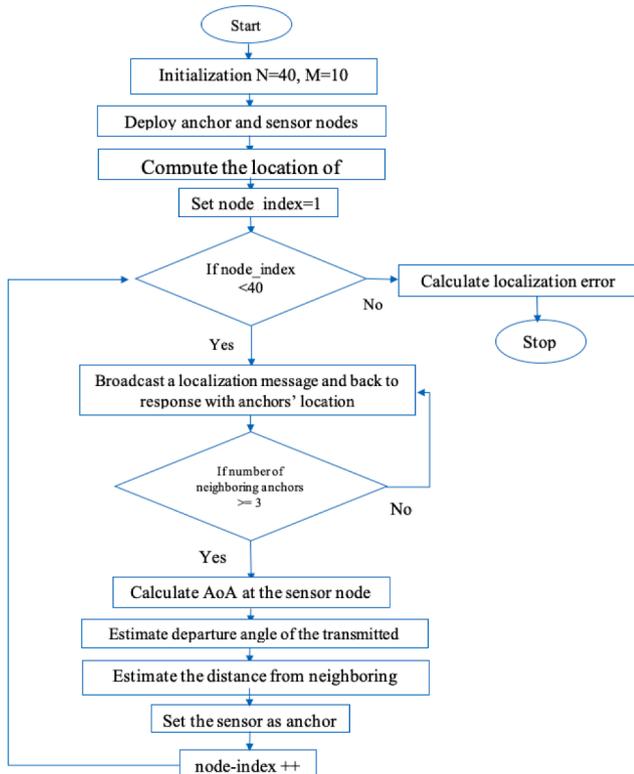
To have accurate position estimation, we develop a minimax estimation approach that minimizes the maximum estimation error as below:

$$\min_{y_1, y_2, \ldots, y_M, e_i \, \hat{s}_j, d_{ij}} \max \sum_{j=1}^{N} MSE_j \tag{13}$$

To simplify the notation, we substitute s instead of s_j in the rest of the paper.

Theorem 2. The minimum MSE of the proposed estimator is given by:

$$MSE_{min} = \mathbb{E}(s\hat{s}) - \mathbb{E}(s^2) = \mathbb{E}(\hat{s}^2) - \mathbb{E}(s^2) = \sigma_{\hat{s}}^2 - \sigma_s^2 \tag{14}$$

Proof. See Appendix C. ∎

Without loss of generality, the estimation problem can be expressed as:

$$\hat{s} = \left(Y_j^T \Sigma_w^{-1} Y_j\right)^{-1} Y_j^T \Sigma_w^{-1} \mathbb{D} + w_i \tag{15}$$

where w_i is the Gaussian observation noise vector with covariance matrix Σ_w, $w_i \sim \mathcal{N}(0, \Sigma_w)$.

Theorem 3. Assume that T is a positive definite matrix, $\|sAptCommand2016;_T \leq S_M \forall S_M > 0$, and $\| s \|_T^2 = s^* T s$, If $S_M^2 = \mathcal{K}^* \Sigma_w^{-1} Y (Y^* \Sigma_w^{-1} Y)^{-2} Y^* \Sigma_w^{-1} \mathcal{K}$, the original minimax optimization problem in (9) can be written as a standard SDP as follows:

$$\min_{\lambda, D, c} c$$

$$\text{s.t.} \begin{bmatrix} c - S_M^2 \lambda & \mathcal{K}^* \\ \mathcal{K} & I \end{bmatrix} \geq 0$$

$$\begin{bmatrix} \lambda I & T^{-\frac{1}{2}}(I - DY)^* \\ (I - DY)T^{-\frac{1}{2}} & I \end{bmatrix} \geq 0 \tag{16}$$

where $\mathcal{K} = vec(D\Sigma_w^{1/2})$.

Proof. See Appendix D. ∎

In the following section, we will analyze the performance of the proposed estimation method using the Fisher information (FI).

Assumption 1. We assume $s_1, s_2, \ldots$ as uniform independent distributed random points on the network grid G in the Euclidean space E. Let N be a positive integer such that $\{s_1, \ldots, s_N\}$ is known as the uniform N-point process on G which is defined as $\chi_N(G)$ such that:

$$s = (s_1, \ldots, s_N) \sim f_{X(s_j)} = \frac{1}{N}, \; j = 1, 2, \ldots, N \tag{17}$$

We also assume that anchors are located according to a homogeneous Poisson point process (PPP) with intensity λ_M which is independent of $\{s_1, \ldots, s_N\}$. Let $\{a_1, \ldots, a_M\}$ be the Poisson point process and $Y(\lambda_M)$ be a Poisson random variable such that:

$$a = (a_1, \ldots, a_M) \sim f_{Y(a_i)} = \frac{exp^{-(\lambda_M t)}(\lambda_M t)^{a_i}}{(a_i)!}, \; i = 1, 2, \ldots, M \tag{18}$$

The problem is to estimate sensors' location in order to accuracy improvement and bias in the estimation. We can approximate the sensors' location using anchors' location as follows:

$$P(s_j | Y = a_i) = \frac{P(S = s_j \bigcap Y = a_i)}{P(Y = a_i)}$$

$$= \frac{P(S = s_j \bigcap Y = a_i)}{P(Y = y_i \bigcap S = s_1) + \ldots + P(Y = a_i \bigcap S = s_N)} \tag{19}$$

According to Bayes' rule, the conditional probability can be expressed as:

$$P(s_j | Y = a_i) = \frac{P(Y = a | S = s_j).P(S = s_j)}{P(Y = a | S = s_1).P(S = s_1) + \ldots + P(Y = a | S = s_N).P(S = s_N)} \tag{20}$$

Definition 1. Assume $\Phi(y)$ is a regression function on y, the location of each sensor node can be approximately calculated as $\hat{s} = \Phi(y)$ in order to $MSE = \mathbb{E}\{\|\hat{s} - sAptCommand2016;^2\}$ is also minimized.

Theorem 4. The location of each sensor can be estimated as below:

$$\hat{s}_j = \mathbb{E}(s_j | a_i) \tag{21}$$

Proof. See Appendix E. ∎

However, some limitations of the proposed approach are that the propagation speed in underwater channel is highly variable, depending on the depth, temperature, and salinity of the water. Therefore, we require to measure propagation speed through exchanging packets between floating buoys on the seabed and the water surface to obtain more accurate localization estimation. Moreover, we cannot assume time synchronization between anchor nodes since they are usually submerged. Thus, we need a solution for time synchronization since a long propagation delay in the underwater environment makes it impossible to ignore clock skew.

Now, we develop a distributed algorithm for AoA/RSS-based localization in UW-IIoT. In this algorithm, each sensor node collects the location information of its neighbor anchors. A sensor then calculates approximately its location using AoA observations and RSS measurements. The sensor evaluates the estimation quality by the MSE criterion. To take mobility into account, the sensor updates its location using the priori location estimate and the current measurement. The algorithm determines CRLB as a lower bound on the estimation error under the noisy distance measurements to achieve localization accuracy. Therefore, the algorithm is repeated to converges the CRLB and all sensor nodes are localized. Algorithm 1 presents the pseudo-code of the distributed localization method.

5. Performance evaluation

In this section, we employ CRLB to derive an error bound of the proposed localization method. CRLB defines a lower bound on the variance of the proposed estimator using the Fisher Information Matrix. According to CRLB, an estimator would be considered efficient if the variance of the estimator is as high as the inverse of FIM. The efficiency [43] of the unbiased estimator $\hat{s}$ is given by:

$$eff(\hat{s}) = \frac{I^{-1}(\hat{s})}{var(\hat{s})}, eff(\hat{s}) \leq 1 \tag{22}$$

where $I(s)$ denotes the FI and it is expressed as follows:

$$I(s) = n \, \mathrm{E}\left[\left(\frac{\partial \log f(Y; \hat{s})}{\partial \hat{s}}\right)^2\right] \tag{23}$$

where $\log f(Y; \hat{s})$ denotes the log-likelihood function, $Y = [y_1 y_2 \ldots y_M]^T$ is the vector of observable anchor nodes' locations and $f(Y; \hat{s})$ states the probability density function. When $\log f(Y; \hat{s})$ is twice differentiable, we can rewrite (23) as below:

$$I(s) = -n \, \mathrm{E}\left[\frac{\partial^2 \log f(Y; \hat{s})}{\partial \hat{s}^2}\right] \tag{24}$$

Thus, each estimator which achieves this lower bound is considered efficient. The CRLB lower bound is derived as:

$$CRLB_s = -[I(s)]_{ij}^{-1} \tag{25}$$

in which the elements of the Fisher information matrix for each sensor i

can be calculated as follows

$$[I(s)]_{ij} = \begin{bmatrix} \displaystyle\sum_{i=1}^{M} \frac{10\ \gamma_{ij}^2 \left(s_{jx} - a_{ix}\right)^2}{\ln 10 d_{ij}^4 \eta_i^2} & \displaystyle\sum_{i=1}^{M} \frac{\gamma_{ij}^2 \left(s_{jx} - a_{ix}\right)\left(s_{jy} - a_{iy}\right)}{d_{ij}^4 \eta_i^2} \\ \displaystyle\sum_{i=1}^{M} \frac{\gamma_{ij}^2 \left(s_{jx} - a_{ix}\right)\left(s_{jy} - a_{iy}\right)}{d_{ij}^4 \eta_i^2} & \displaystyle\sum_{i=1}^{M} \frac{\gamma_{ij}^2 \left(s_{jy} - a_{iy}\right)^2}{d_{ij}^4 \eta_i^2} \end{bmatrix} \quad (26)$$

On the other hand, the minimum MSE can be expressed as:

$$MSE_{\min,s} = trace\ \{CRB_s\} \quad (27)$$

Since MSE matrix can be measured by FIM inequality, we can evaluate the error bound on our approach. Therefore, it can be concluded that if the proposed localization method achieves the CRLB's lower bound, it achieves the lowest possible mean squared error.

5.1. Complexity analysis

In this section, we investigate the computational complexity of the proposed approach. The main computational complexity of our algorithm is bounded by the SDP solution [43]. Thus, the number of arithmetic operations to compute interior points in solving a localization problem with $n = M + N$ nodes is derived as:

$$O(1)\left(1 + \sum_{k=1}^{K} m_k^{sd}\right)^{1/2} n\left(n^2 + n\sum_{k=1}^{K} m_k^{sd^2} + \sum_{k=1}^{K} m_k^{sd^3}\right) \quad (28)$$

Where K identifies the number of SDC constraints, m_k^{sd} denotes the size of diagonal blocks of SDP diagonal matrices. it is worth mentioning that all sub-problems of the proposed approach can be easily transformed into the SDP form. Therefore, the worst-case complexity of the proposed localization algorithm is bounded by $O(n^3)$. We also investigated the complexity of two other related algorithms in comparison with the proposed approach in Table 2.

In addition, from the space complexity point of view, the presence of $(D + 1)$ direct localizable neighbors are necessary for a sensor to be localizable in $(t + 1)$ iterations for D dimensional space. It follows that the $(D + 1)$ neighbors must be localized in $(t - 1)$ communication rounds to the sensor can be localized within t rounds. If any h hop neighbor may contribute to the node's localization, they should be localized within $(t - h)$ iterations. Thus, if the node needs to be localized over t iteration, then the $(D + 1)$ direct neighbors should be found in those rounds.

5.2. Hardware equipment for real-time experiment

To validate the feasibility of the proposed approach, real-time experiment can be conducted at sea. The underwater hardware equipment can be included the sonar camera system as a sensor device to gather depth information for fish metric measurements, such as fish length and fish number. The device uses multiple sound waves to send information about fish to the scene via its beam. In this way, it is able to capture depth information from an actual environment. While sonar devices offer wide coverage, they lack color and texture information. More precisely, sonar provides images of objects that are very different from optical images by using depth information. In contrast to sonar cameras, stereo cameras address this limitation. A combination of these two devices can provide a better view of underwater fish. Furthermore, LoRa or BLE can be used for water surface and underwater

Table 2
Complexity analysis.

Approach	Complexity
[28]	$O(n^2)$
[33]	$O(n^{3.5})$
The proposed algorithm	$O(n^3)$

communication. However, LoRa is more stable than BLE [46] since LoRa [47] and [48] provides low-power long-range connectivity, however, BLE offer low-power short-range connectivity.

6. Experimental results

In this section, we present the performance evaluation of the proposed approach with the scheme in [28] labeled as EHL and an efficient RSS localization algorithm in [32] known as E-RSS. All of the performance evaluations were carried out by the MATLAB package CVX and the SeDuMi solver. The numerical results were obtained from $M_c = 1800$ independently Monte Carlo run. The RSS measurements were calculated based on Eq. (1) in which $\rho = 0.39 S/m$. We set θ_1 and θ_2 based on uniform distributed in [0,] in our simulation experiments. We also adjusted the path loss (Γ_{ij}) in the range of -100 dB to 0 dB and varied the noise variance σ^2 from 0.1 to 0.6 in experiments [49]. For simplicity, the noise variance for all sensors is considered the same $\sigma_i^2 = \sigma^2$. The key simulation parameters are listed in Table 3.

We consider a 2-D localization scenario with $N = 40$ sensor nodes and $M = 10$ anchor nodes in which the anchor and sensor nodes are randomly distributed in an area of $100\ m \times 100$ m. A tradeoff analysis was conducted among localization coverage, the node density, communication cost and the estimation error. We set the number of underwater sensor nodes to $N = 40$ in order to examine localization coverage and localization accuracy in a large-scale underwater scenario. We also adjusted the number of anchor nodes to $M = 10$ because it is the critical value of M for our setting. More precisely, when the value of M increases up to 10, the estimation error will be reduced and the localization coverage will be grown. However, the estimation error and the localization coverage are relatively stable for larger value of $M > 10$ while the average communication cost will grow speedily. Increasing M beyond the critical value (i.e., $M > 10$) will only rise communication costs without bringing any profits. As such, a careful choice of M must be made in practice based on the network environment. These parameters may differ for different networks. Fig. 5 displays the smart node's deployment.

We use the root mean square error (RMSE) metric to evaluate the performance of the existing approaches. The RMSE is expressed as:

$$RMSE = \sqrt{\sum_{i=1}^{M_c} \frac{\| s_i - \hat{s}_i \text{AptCommand2016}^2}{M_c}} \quad (29)$$

Fig. 6 demonstrates the RMSE of the proposed algorithm and the considered schemes versus different values of the noise variance σ^2.

We varied the range of σ^2 from 0.1 to 0.6. The results show that the positioning error is less than 3 m for existing approaches under the different values of σ^2. Furthermore, there is a performance gap between our method and the other approaches of approximately 1.2 m. Furthermore, the analytical CRLB of our approach is also depicted. Although all three methods achieve good performance in terms of estimation accuracy, the proposed approach outperforms the considered schemes. As it can be seen, the CRLB is a realistic bound for an unbiased estimator and validates the theoretical results very well.

We analyze the performance of the proposed approach in terms of estimation accuracy under different numbers of anchor nodes in Fig. 7.

Table 3
Simulation parameter.

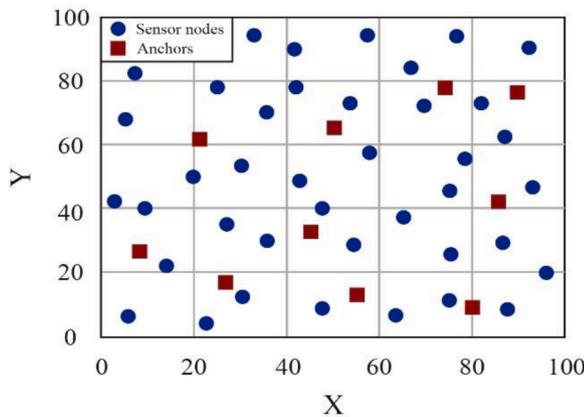| Description	Parameter	Value
Water depth	h	40m
Communication radius of anchor nodes	R_j	20m
Communication radius of sensor nodes	R_i	10m
Transmission power	P_i^{tr}	32 dBm
Path-loss exponent	γ	2
Reference distance	d_0	1m

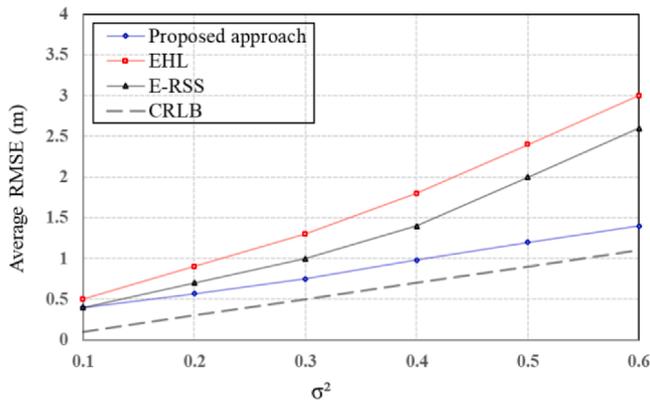**Fig. 5.** The network deployment scenario.

Fig. 6. The RMSE performance comparison between theoretical CRLB of the proposed algorithm and simulation results for all methods under different σ^2.
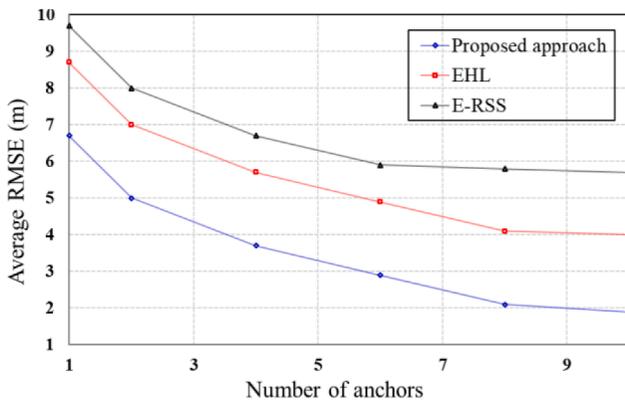

Fig. 7. Average RMSE for existing methods under different number of anchors.

The experiments were run for various number of anchors from 1 to 10. As expected, the estimation accuracy is dramatically enhanced by involving more anchor nodes in the localization process. For example, our approach yields the average RMSE= 6.729 m and RMSE= 1.953 m for the number of anchors $M = 1$ and $M = 10$. Whereas, the EHL method achieves the average RMSE= 8.715 m and RMSE= 4.173 m and the E-RSS scheme obtains the RMSE= 9.829 m and RMSE= 5.713 m on average in the same condition. The results verify superiority of the proposed method in terms of RMSE performance. However, it is worth mentioning that increasing the number of anchor nodes increases the implementation cost in network. We also plot the impact of the path-loss exponent on the MSE of estimation for $N = 40$ and $M = 7$ in Fig. 8. We
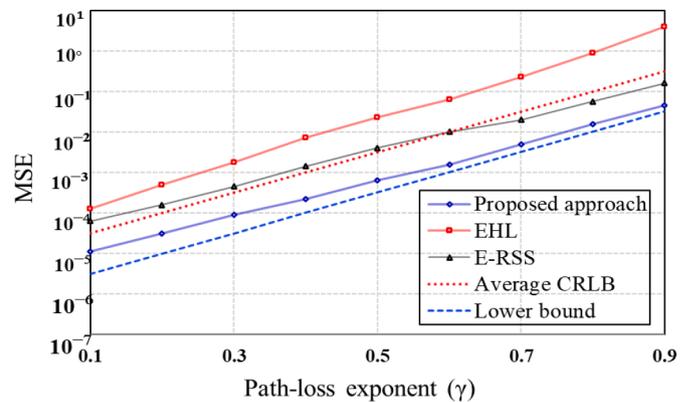

Fig. 8. Performance comparison between theoretical MSE of proposed approach and simulation results of the existing algorithms for $N = 40$, $M = 7$, and $\sigma^2 = 0.4$.

decrease the number of anchors to examine its impact under different path loss on the localization error. We consider different path-loss exponent values ranging from 0.1 to 0.9 for $\sigma^2 = 0.4$ and different distances from 2 m to 11 m. The Figure shows that as the number of actively participating anchors declines, sensors are localized in a shorter path because the received signal strength accuracy depends on factors such as the number of anchors, and distribution of anchors. Fewer anchor nodes means receiving noisy RSS from distant neighbor anchors with large path loss. The higher the path losses, the lower the received signal power. For example, when $\gamma = 0.3$ with the variance 0.4 and the distance ranges up to 8 m, the MSE value of our estimator is less than 10^{-4} m while the MSE value is less than 10^{-2} m for $\gamma = 0.7$ in the same condition. According to the results, when the value of γ is too small (e.g., $\gamma = 0.2$) all approaches achieve good results in terms of position estimation, in contrast, the path-loss exponent effect is very considerable in $\gamma = 0.6$ on estimation error for the all considered methods. According to Figs. 6 and 7, the RMSE decreases with the larger number of anchor nodes. The reason is when the number of neighboring anchors increases the localization accuracy is enhanced and RMSE is reduced. On the other hand, when the noise variance grows, the localization error is increased and RMSE falls. Nevertheless, there is a threshold for the number of the anchors. As the number of anchors increase the communication cost rises results in energy depletion of sensor nodes. According to simulation results, the localization accuracy falls for $M<7$ and communication cost grow for $M>10$. As a matter of fact, the algorithm reaches the best performance in terms of localization accuracy and communication cost when the number of anchors is set to 10.

Table 4 provides the localization results and the estimation error of a randomly selected sensor node under various anchor nodes in different iterations. At each iteration, the algorithm selects different anchors and estimates the position of unlocalized nodes and refines the estimated location of localized sensors using messages from their neighbor anchors. The algorithm converged in 25 where the position of all nodes is determined and the estimation error was minimized.

The impact of sensors' communication range on the localization error is depicted in Fig. 9. We change the sensing radius of sensors from 2 to 11 m while the deployment area is kept the same. The anchor nodes proportion is considered 15% at node density 40 with $d_0 = 1m$, $\gamma = 0.3$, $\sigma^2 = 0.2$. Apparently, as the communication range of sensors increases, the positioning error is reduced. When the sensing range of nodes is short, the number of hops is increased which results in the increase in position measuring and high positioning error subsequently. It can be seen that all methods obtain remarkable improvements in terms of the estimation accuracy, however, the proposed method produces much better results in error reduction. Furthermore, the ratio of the localizable sensors increases significantly with increasing the sensing radius of sensors (Fig. 10).

Table 4
Localization results of a typical sensor.

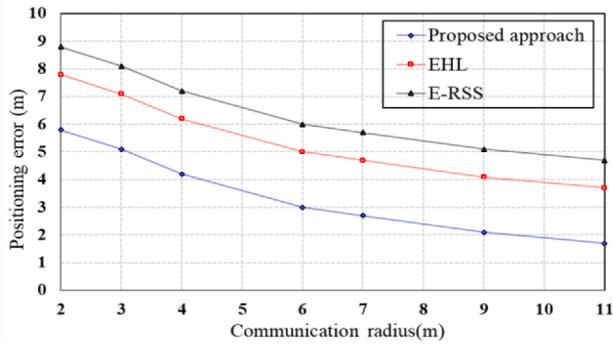| Iteration	Anchor nodes	Estimated location	Actual location	Estimation error
1	1,3,6,9,13,17,23,26,34,39	(25.61,14.99)	(48.04,77.05)	75.07
5	2,7,8,12,17,21,26,33,38,40	(57.05,28.01)	(48.04,77.05)	59.83
10	1,3,7,13,15,19,22,25,29,37	(52.35,26.37)	(48.04,77.05)	56.50
15	3,5,9,13,17,21,26,34,39,40	(7.17,73.12)	(48.04,77.05)	33.82
18	2,4,7,9,12,17,23,25,29,35	(41.48,66.18)	(48.04,77.05)	13.43
25	1,3,9,13,17,21,26,29,33,39	(45.42,78.97)	(48.04,77.05)	3.32

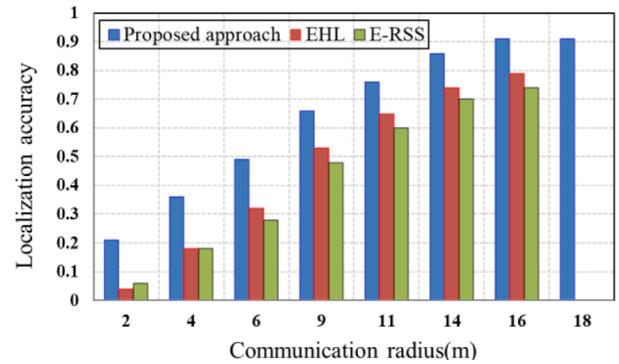**Fig. 9.** Effect of communication range on the localization error at $\gamma = 0.3$, $\sigma^2 = 0.2$.

Fig. 12. Localization accuracy under different communication radius of sensors.

The empirical CDF of estimation error can be defined as [43]:

$$CDF(\varepsilon) = \Pr(estimation\ error\ \leq\ \varepsilon) = \frac{\sum_{k=1}^{K}\sum_{i=1}^{N}F\left(\parallel exp_i^k \parallel - \varepsilon\right)}{NK}$$
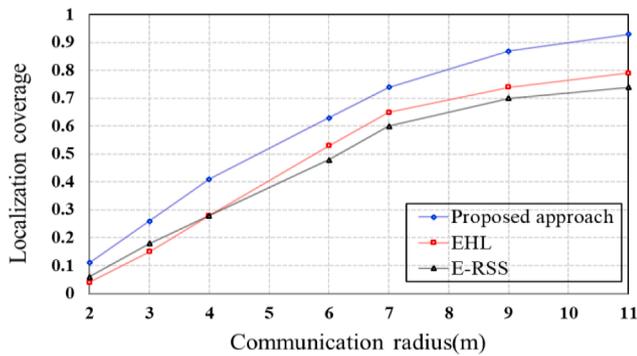
where

Fig. 10. Localization coverage ratio under different communication ranges.

The large the communication radius, the more sensors would be captured. For example, when the communication radius reaches 10 m, the ratio of the localizable nodes is 91% whereas the localization coverage is 58% when the sensing range is 5 m.

Fig. 11 displays the cumulative density function (CDF) of estimation error for the existing approaches.
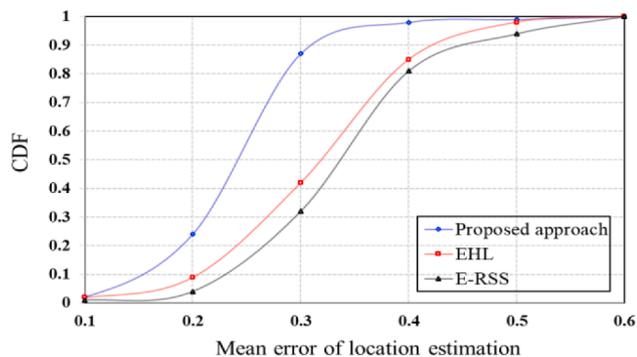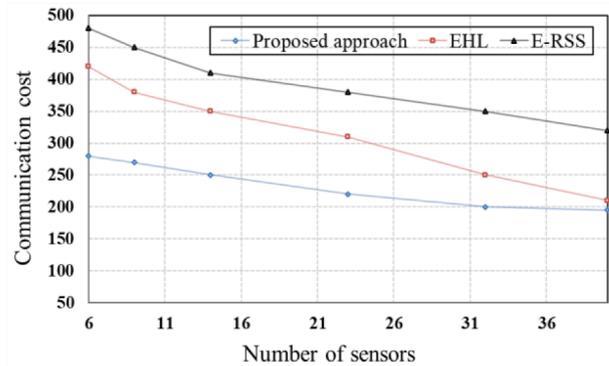

Fig. 11. Cumulative density function (CDF) of estimation error for the existing algorithms under $N = 40$, $M = 8$, $\gamma = 0.3$, and $\sigma^2 = 0.6$.
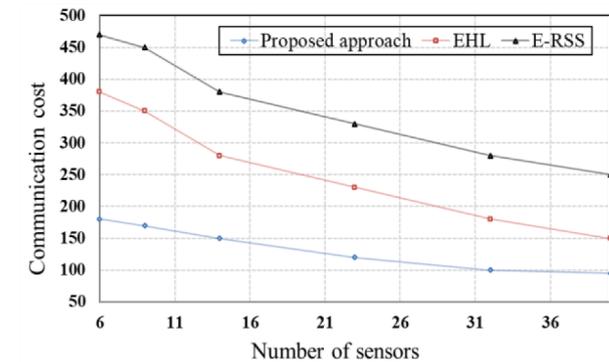

a) Anchor percentage=10%

b) Anchor percentage=20%

Fig. 13. Communication cost under different node density and various anchor percentage.

Table 5
Comparison of the proposed scheme and previous work.

Approach	Localization accuracy	Localization coverage	Communication cost	Positioning error	Sync	Energy efficient
[28]	93%	89%	13%	7%	Yes	Yes
[33]	84%	97%	7%	16%	No	No
The proposed algorithm	97%	94%	11%	3%	No	No

Algorithm 1
RSS-based localization algorithm.

Initialize ρ, D
Set $N = 40$, $M = 10$
For all sensor nodes
Repeat
Choose randomly an anchor node a_i
   Set P_i, R_i, α_i, β_j, L_{ij}
   Calculate d_{ij}
Find $\widehat{s}_j = \arg \min_{x \in X} \alpha_j d_{ij}^2 + \beta_j d_{ij} - 1$
Evaluate $MSE = \{(\widehat{s}_j - s_j)(\widehat{s}_j - s_j)^T\}$
Calculate CRLB according to (25) and (26)
Until $MSE_{min,s} = trace\{CRB_s\}$
Update the current location of the sensor based on the previously known location
   information and current measurement
$\widehat{s}_j(t) = s_j(t-1) - (\mathbb{D}^T\mathbb{D} + \delta I)^{-1}\mathbb{D}(\widehat{d}_{ij} - \Delta(\widehat{s}_j(t-1)))$
Update the distance matrix $\mathbb{D}$
   End for user loop
Return $\mathbb{D}$

$$F(x) = \begin{cases} 0 & x \leq x_1 \\ \dfrac{k}{N} & x_k \leq x \leq x_{k+1} \\ 1 & x \geq x_N \end{cases} \tag{30}$$

in which k denotes the kth estimate, N is the number of nodes, and $\| e_i^k \|$ identifies the Euclidean norm of the kth estimate error of node i. The experiments are repeated 60 times and measure the sum of prediction errors made under the same conditions. As we can see, the estimation error created by the proposed approach does not surpass 35 cm, whereas the position error is about 45 cm for two other algorithms. This fact verifies the superiority of the proposed algorithm by approximately 11% estimation error reduction compared to the other related methods.

Fig. 12 plots the impact of communication range of sensor nodes on the localization accuracy.

When the communication range increases, the localization accuracy grows due to node connectivity enhancement. Simulation results verifies that even if the signal strength is compensated, localization accuracy will be decreased if node connectivity reduced. The communication radius can improve the network connectivity by up to 85%, results in impressive enrichment in localization accuracy.

We investigate the impact of number of anchors (node density) on the communication cost of the existing methods in Fig. 13. Clearly, EHL and E-RSS schemes introduce larger communication cost than the proposed approach even though when the node density is small. This is

because, they exchange beacon messages even when the network is sparse to localize themselves. However, the average communication cost of the proposed scheme is very small since in our method, only nodes with known locations broadcast messages and other nodes keep silent. Compared with two other methods, our scheme can always achieve much lower communication cost. It can be also seen that the average communication cost of our scheme decreases with the increase of anchor percentage. This is due to that fact that our scheme can achieve more network connectivity that helps to find more reference nodes much faster without exchanging too many beacon messages.

We finally, summarize the overall improvements of the proposed method compared to previous work in the Table 5.

7. Conclusion

In this paper, we proposed an accurate RSS-based localization algorithm for smart fishing in UW-IIoT. First, we modeled the localization problem under noisy observations. We then developed a minimax approach to minimize the maximum estimation error. Furthermore, the problem was converted to SDP in order to be solved globally in polynomial time. The CRLB as a benchmark was derived in order to determine a lower bound on the MSE of the proposed estimator. The proposed approach estimates the location of fish in order to help fishermen catch fish faster and easier. Moreover, such smart fishing optimizes energy consumption and saves fuel costs. The experimental results verified the superior performance of the proposed method in terms of both estimation accuracy and localization coverage. As a future research direction, we will study underwater localization problem with imperfect clock synchronization between anchor and sensor nodes. Due to the unknown propagation delay, we need to measure clock synchronization errors in the received signal analysis. Designing a jointly propagation delay and node location estimation approach can reduce the localization estimation error. Moreover, we will evaluate and validate the performance of the proposed localization algorithm using real testbed (Algorithm 1).

Declaration of Competing Interest

The authors declare that they have no known competing financial interests or personal relationships that could have appeared to influence the work reported in this paper.

Data availability

No data was used for the research described in the article.

Appendix A

Proof of Theorem 1
Proof. According to the definition of d_{ij}, we have

$$d_{ij} = \sqrt{\sum_{i=1}^{M} \left(s_{rj} - a_{ri} \right)^2} \tag{A.1}$$

Therefore, we express the error function as below:

$$\Delta \widehat{s}_j = \sum_{i=1}^{M} \left(\widehat{d}_{ij} d_{ij} \right)^2 \tag{A.2}$$

Due to $\frac{\partial \Delta \widehat{s}_j}{\partial s_{rj}} = 0$, $r = 1,...,N$, we have

$$\sum_{i=1}^{M} 2\widehat{d}_{ij} d_{ij} \left(\frac{s_{rj} - a_{ri}}{d_{ij}} d_{ij} + \frac{s_{rj} - a_{ri}}{d_{ij}} \widehat{d}_{ij} \right) = 0 \tag{A.3}$$

In other words, we can rewrite the above equation as:

$$s_{rj} \sum_{i=1}^{M} \left(\widehat{d}_{ij} d_{ij} + \widehat{d}_{ij}^2 \right) - \sum_{i=1}^{M} a_{ri} \left(\widehat{d}_{ij} d_{ij} + \widehat{d}_{ij}^2 \right) = 0 \tag{A.4}$$

So, the following results is driven

$$s_{rj}^* = \frac{\sum_{i=1}^{M} A_r \widehat{d}_{ij} (d_{ij} + \widehat{d}_{ij})}{\sum_{i=1}^{M} \widehat{d}_{ij} (d_{ij} + \widehat{d}_{ij})}, r = 1,...,N \tag{A.5}$$

Taking second-order derivation of the error function shows the coordinates of the vector $\Delta \widehat{s}_j$ take the minimum values at the point $(s_{1j}^*, s_{2j}^*, ..., s_{Nj}^*)$ as follows:

$$\frac{\partial}{\partial s_{rj}} \left(\frac{\partial \Delta \widehat{s}_j}{\partial s_{rj}} \right) = \sum_{i=1}^{M} \left(\widehat{d}_{ij} d_{ij} + \widehat{d}_{ij}^2 \right) \rangle 0 \tag{A.6}$$

And this completes the proof. ∎

Appendix B

Proof of Proposition 1
We set $d_0 = 1$ and substitute $\|s_j - a_i\| = d_{ij}$. Dividing both sides of the Eq. (1) by 10γ gives:

$$\frac{P_i - P_0}{10\gamma} + \log_{10} d_{ij} = \frac{\eta_i}{10\gamma} \tag{B.1}$$

We raise both sides of the above equation using the power of 10 to eliminate the log therefore we have:

$$10^{\frac{P_i - P_0}{10\gamma}} \times d_{ij} = 10^{\frac{\eta_i}{10\gamma}} \tag{B.2}$$

Since the shadowing effect can be neglected in a deep ocean environment, the value of $\eta_i \ll 10\gamma/\ln 10$ is small enough. Thus, using first-order Taylor expansion, we can obtain

$$10^{\frac{\eta_i}{10\gamma}} \simeq 1 + \frac{\ln 10}{10\gamma} \eta_i \tag{B.3}$$

Substituting (B.3) into (B.2) leads to

$$\beta_j \times d_{ij} = 1 + \frac{\ln 10}{10\gamma} \eta_i \tag{B.4}$$

In which $\beta_j = 10^{\frac{P_i - P_0}{10\gamma}}$. More precisely, we have

$$\alpha_j d_{ij}^2 + \beta_j d_{ij} - 1 = e_{ij} \tag{B.5}$$

Where $\alpha_j = \frac{\beta_j \ln 10}{10\gamma}$ and $e_{ij} = \frac{\ln 10}{10\gamma} \eta_i$.
Without loss of generality, we can formulate the localization problem as below:

$$\widehat{s}_j = \arg \min_{s_j} \alpha_j d_{ij}^2 + \beta_j d_{ij} - 1 \tag{B.6}$$

In the other world, the above equation can be rewritten as:

$$\min_{s_j} \sum_{j=1}^{N} \left| \alpha_j d_{ij}^2 + \beta_j d_{ij} - 1 \right| \tag{B.7}$$

Using a slack variable $z_{ij} \geq 0$, we transform the above optimization problem as follows:

$$\min_{s_j, d_{ij}, z_{ij}} z_{ij}$$

$$\text{s.t.} \; -z_{ij} < \alpha_j d_{ij}^2 + \beta_j d_{ij} - 1 < z_{ij}$$

$$d_{ij}^2 = \| s_j - a_i \|_2^2$$

$$D = \begin{bmatrix} s_j^T & 1 \end{bmatrix} \begin{bmatrix} I^T & -a_i \\ -a_i^T & a_i^T a_i \end{bmatrix} \begin{bmatrix} s_j \\ 1 \end{bmatrix} = \text{Trace} \, [SA] \tag{B.8}$$

where $\begin{bmatrix} I^T & -a_i \\ -a_i^T & a_i^T a_i \end{bmatrix} = A_j$ identifies the known locations from the anchor node a_i. Due to S and D are positive semidefinite, $rk(S) = rk(D) = 1$ where rk $(\cdot)$ denotes the rank of a matrix. Thus, we can reformulate the problem (B.8) as below:

$$\min_{S,D,z_{ij}} \sum_{j=1}^{N} z_{ij}$$

$$\text{s.t.} -z_{ij} < \alpha_j D + \beta_j D - 1 < z_{ij}$$

$$D = \text{Trace}[SA]$$

$$S \geq 0, \ D \geq 0$$

$$[S]_{(N+1)(N+1)} = [D]_{(M+1)(M+1)} = 1 \tag{B.9}$$

Consequently, the optimization problem in (B.9) is an SDP-based problem that is globally solved by $[\widehat{S}]_{(N+1)(N+1)}$. So the proposition holds. ∎

Appendix C

Proof Of Theorem 2
According to the MSE definition, we can write

$$MSE_{min} = \mathbb{E}\left\{\left\|\widehat{s} - s\right\|^2\right\} = \mathbb{E}\{(\widehat{s} - s)s\} - \mathbb{E}\{(\widehat{s} - s)\widehat{s}\} \tag{C.1}$$

Due to orthogonality, we have $\mathbb{E}\{(\widehat{s} - s)\widehat{s}\} = 0$. Thus,

$$MSE_{min} = \mathbb{E}(s\widehat{s} - s^2) = \mathbb{E}(s\widehat{s}) - \mathbb{E}(s^2) \tag{C.2}$$

It is well understood that $\mathbb{E}(s\widehat{s}) = \mathbb{E}(\widehat{s}^2)$. Now, we can rewrite

$$MSE_{min} = \mathbb{E}(\widehat{s}^2) - \mathbb{E}(s^2) \tag{C.3}$$

Clearly, $\mathbb{E}(s) = \mathbb{E}(\widehat{s})$. Therefore, it can be concluded that

$$MSE_{min} = \mathbb{E}\mathbb{E}(\widehat{s}^2) - \mathbb{E}(s^2) - (\mathbb{E}(s))^2 + (\mathbb{E}(\widehat{s}))^2 = \sigma_{\widehat{s}}^2 - \sigma_s^2 \tag{C.4}$$

So, the theorem holds. ∎

Appendix D

Proof Of Theorem 3
We can rewrite (9) as below:

$$\min_{D} \max_{\|s\|_T \leq S_M} \{s^*(I - DY)^*(I - DY)s + Tr(D\Sigma_w D^*)\} \tag{D.1}$$

The worst parameters can be specified as the solution to the above equation:

$$\max_{\|s\|_T \leq S_M} s^*(I - DY)^*(I - DY)s \tag{D.2}$$

By replacing $v = T^{\frac{1}{2}} s$, we can write:

$$\max_{s^* T s \leq S_M} s^*(I - DY)^*(I - DY)s = \max_{v^* v \leq S_M^2} v^* T^{-\frac{1}{2}}(I - DY)^*(I - DY)T^{-\frac{1}{2}}v = S_M^2 \lambda_{max} \tag{D.3}$$

where λ_{max} denotes the maximum eigenvalue in $T^{-\frac{1}{2}}(I - DY)^*(I - DY)T^{-\frac{1}{2}}$. Therefore, we can state λ_{max} as the solution to

$$\min_{\lambda} \lambda$$

$$\text{s.t.} T^{-\frac{1}{2}}(I - DY)^*(I - DY)T^{-\frac{1}{2}} \leq \lambda I \tag{D.4}$$

Using (D.3) and (D.4), the problem in (D.1) can be written as below:

$$\min_{D, \lambda}\{Tr(D\Sigma_w D^*) + S_M^2 \lambda\} \tag{D.5}$$

which is equivalent to the following according to (D.4):

$$\min_{\lambda,D,c} c$$

$$\text{s.t.} Tr(D\Sigma_w D^*) + S_M^2 \lambda \leq c$$

$$T^{-\frac{1}{2}}(I - DY)^*(I - DY)T^{-\frac{1}{2}} \le \lambda I \tag{D.6}$$

Thus, we showed that the original problem is formulated as an SDP which can be solved very efficiently in polynomial time.

Using $\mathscr{K} = vec(D\Sigma_{w}^{1/2})$, we rewrite (D.6) as follows:

$$\mathscr{K}^*\mathscr{K} + S_M^2\lambda \le c \tag{D.7}$$

However, to solve an SDP problem, the constraints need to be in form of linear matrix inequality (LMI). Using Schur's complement, we can express the constraints (D.6) as LMIs in the variables λ, D, and α. Therefore, we have:

$$\begin{bmatrix} c - S_M^2\lambda & \mathscr{K}^* \\ \mathscr{K} & I \end{bmatrix} \ge 0 \tag{D.8}$$

and

$$\begin{bmatrix} \lambda I & T^{-\frac{1}{2}}(I - DY)^* \\ (I - DY)T^{-\frac{1}{2}} & I \end{bmatrix} \ge 0 \tag{D.9}$$

And this completes the proof. ∎

Appendix E

Proof of Theorem 4

Obviously, the localization MSE for a typical node is given by

$$MSE = \mathbb{E}\{\| \widehat{s}_j - s_j \|^2\} = MSE = \mathbb{E}\{\| \Phi(a_i) - s_j \|^2\} = \sum_{j=1,2,\ldots,N}\sum_{i=1,2,\ldots,M} (\widehat{s}_j - s_j)^2 P(s_j, a_i)$$

$$= \mathbb{E}\left\{\mathbb{E}\left((\widehat{s}_j - s_j)^2 \big| a_i\right)\right\} = \sum_{i=1,2,\ldots,M} P(a_i)\left[\sum_{j=1,2,\ldots,N} (\widehat{s}_j - s_j)P(s_j | a_i)\right] \tag{E.1}$$

To minimize MSE we can write the following:

$$L = \sum_{j=1,2,\ldots,N} (\widehat{s}_j - s_j)^2 P(s_j | a_i) = \sum_{j=1,2,\ldots,N} (\Phi(a_i) - s_j)^2 P(s_j | a_i)$$

$$= \mathbb{E}\left(s_j^2 \big| a_i\right) - 2\widehat{s}_j\mathbb{E}(s_j | a_i) + \widehat{s}_j^2 \frac{\partial L}{\partial \widehat{s}_j} = 0 \Rightarrow \widehat{s}_j = \mathbb{E}(s_j | a_i) : \forall s \tag{E.2}$$

Thus,

$$\widehat{s}_j = \mathbb{E}(s_j | a_i) \tag{E.3}$$

And this completes the theorem. ∎

References

[1] E. Sisinni, A. Saifullah, S. Han, U. Jennehag, M. Gidlund, Industrial internet of things: challenges, opportunities, and directions, IEEE Trans. Ind. Inform. 14 (11) (2018) 4724–4734.

[2] E.C. Liou, C.C. Kao, C.H. Chang, Y.S. Lin, C.J. Huang, Internet of underwater things: challenges and routing protocols, in: Proceedings of the IEEE International Conference on Applied System Invention (ICASI), 2018, pp. 1171–1174.

[3] M.C. Vuran, A. Salam, R. Wong, S. Irmak, 'Internet of underground things: sensing and communications on the field for precision agriculture, in: Proceedings of the IEEE 4th World Forum Internet Things (WF-IoT), 2018, pp. 586–591.

[4] J.W. Choi, A.V. Borkar, A.C. Singer, G. Chowdhary, Broadband acoustic communication aided underwater inertial navigation system, IEEE Robot. Autom. Lett. 7 (2) (2022) 5198–5205.

[5] K.M. Awan, P.A. Shah, K. Iqbal, S. Gillani, W. Ahmad, Y. Nam, 'Underwater wireless sensor networks: a review of recent issues and challenges, Wirel. Commun. Mob. Comput. 2019 (2019), 6470359.

[6] J. Luo, Y. Yang, Z. Wang, Y. Chen, Localization algorithm for underwater sensor network: a review, IEEE Internet Things J. 8 (17) (2021) 13126–13144.

[7] K. Kumar, K. Pandey, S. Chandra, R. Arya, Evaluation of node-metastasis in sparse underwater acoustic sensor networks for localization under acoustically stratified malicious node conditions, IEEE Access 9 (2021) 169372–169386.

[8] J. Luo, L. Fan, S. Wu, X. Yan, 'Research on localization algorithms based on acoustic communication for underwater sensor networks, Sensors 18 (1) (2018) 67.

[9] X. Zhu, H. Dong, P.S. Rossi, M. Landrø, Time-frequency fused underwater acoustic source localization based on contrastive predictive coding, IEEE Sens. J. (2022).

[10] Y. Lin, H. Tao, Y. Tu, T. Liu, A node self-localization algorithm with a mobile anchor node in underwater acoustic sensor networks, IEEE Access 7 (2019) 43773–43780.

[11] D. Muhammed, M.H. Anisi, M. Zareei, C. Vargas-Rosales, A. Khan, Game theory-based cooperation for underwater acoustic sensor networks: taxonomy, review, research challenges, and directions, Sensors 18 (2) (2018) 425.

[12] T. Islam, Y.K. Lee, A cluster-based localization scheme with partition handling for mobile underwater acoustic sensor networks, Sensors 19 (5) (2019).

[13] R. Zhou, J. Chen, W. Tan, H. Yuan, C. Cai, Sensor selection for hybrid AOA-TOA localization with correlated measurement noise in underwater wireless sensor networks, Wirel. Commun. Mob. Comput. (2022).

[14] R.A. Khalil, N. Saeed, M.I. Babar, T. Jan, S. Din, Bayesian multidimensional scaling for location awareness in hybrid-internet of underwater things, IEEE/CAA J. Autom. Sin. 9 (3) (2021) 496–509.

[15] X.F Wang, G. Han, Y. Sui, H. Qin, EODL: energy optimized distributed localization method in three-dimensional underwater acoustic sensors networks, *Comput. Netw.* 141 (2018) 179–188.

[16] I. Ullah, J. Chen, X. Su, C. Esposito, C. Choi, Localization and detection of targets in underwater wireless sensors using distance and angle-based algorithms, IEEE Access 7 (2019) 45693–45704.

[17] Y.Y Luo, Z. Wang, Y. Chen, M. Wu, A mobility-assisted localization algorithm for three-dimensional large-scale UWSNs, Sensors 20 (2020) 4293.

[18] Y. Yuan, C. Liang, M. Kaneko, X. Chen, D. Hogrefe, Topology control for energy-efficient localization in mobile underwater sensor networks using stackelberg game, *IEEE Trans. Veh. Technol.* 68 (2) (2019) 1487–1500.

[19] H. Huang, Y.R. Zheng, Node localization with AOA assistance in multi-hop underwater sensor networks, Ad Hoc Netw. 78 (2018) 32–41.

[20] S. Misra, T. Ojha, SecRET: secure range-based localization with evidence theory for underwater sensor networks, ACM Trans. Auton. Adapt. Syst. (TAAS) 15 (1) (2021) 1–26.

[21] S. Poursheikhali, H. Zamiri-Jafarian, Received signal strength- based localization in inhomogeneous underwater medium, Signal Process. 154 (2019) 45–56.

[22] R. Mourya, M. Dragone, Y. Petillot, Robust silent localization of underwater acoustic sensor network using mobile anchors, Sensors 21 (3) (2021) 727.

[23] A. Weiss, T. Arikan, H. Vishnu, G. Deane, A. Singer, G. Wornell, A semi-blind method for localization of underwater acoustic sources, IEEE Trans. Signal Process. (2022).

[24] C. Zheng, D. Sun, L. Cai, X. Li, 'Mobile node localization in underwater wireless networks, IEEE Access 6 (2018) 17232–17244.

[25] B. Zhang, H. Wang, L. Zheng, J. Wu, Z. Zhuang, Joint synchronization and localization for underwater sensor networks considering stratification effect, IEEE Access 5 (2017) 26932–26943.

[26] C.D. Demars, M.C. Roggemann, A.J. Webb, T.C. Havens, Target localization and tracking by fusing doppler differentials from cellular emanations with a multi-spectral video tracker, Sensors 18 (2018) 3687.

[27] R. Zhang, J.W. Liu, X.J. Du, B. Li, M. Guizani, AOA-based three-dimensional multi-target localization in industrial WSNs for LOS conditions, Sensors 18 (2018) 2727.

[28] N. Saeed, A. Celik, T.Y. Al-Naffouri, M. Alouini, Localization of energy harvesting empowered underwater optical wireless sensor networks, *IEEE Trans. Wirel. Commun.* 18 (2019) 2652–2663.

[29] S. Chang, Y. Li, Y. He, Y. Wu, RSS-Based Target Localization in underwater acoustic sensor networks via convex relaxation, Sensors 19 (2019) 2323.

[30] J.B. Saif, M. Younis, Underwater Localization using Airborne Visible Light Communication Links, in: Proceedings of the *2021 IEEE Global Communications Conference (GLOBECOM)*, IEEE, 2021, pp. 01–06.

[31] P. Saleheh, Z.J. Hossein, Received signal strength based localization in inhomogeneous underwater medium, Signal Process. 154 (2019) 45–56.

[32] S. Chang, Y. Li, Y. He, W. Hui, Target localization in underwater acoustic sensor networks using RSS measurements, Appl. Sci. 8 (2018) 225.

[33] T. L, N. Nguyen, Y. Shin, An efficient RSS localization for underwater wireless sensor networks, Sensors 19 (2019) 3105.

[34] M. Hosseini, H. Chizari, T. Poston, M.B. Salleh, A.H Abdullah, Efficient underwater RSS value to distance inversion using the lambert function, *Math. Probl. Eng.* 175275 (2014).

[35] X. Shi, G. Mao, B.D. Anderson, Z. Yang, J. Chen, Robust localization using range measurements with unknown and bounded errors, IEEE Trans. Wirel. Commun. 16 (6) (2017) 4065–4078.

[36] H. Lohrasbipeydeh, T.A. Gulliver, RSSD-based MSE-SDP source localization with unknown position estimation bias, IEEE Trans. Commun. 69 (12) (2021) 8416–8428.

[37] M.S. Costa, S. Tomic, M. Beko, An SOCP estimator for hybrid RSS and AOA target localization in sensor networks, Sensors 21 (5) (2021) 1731.

[38] R. Diamant, R. Francescon, A graph localization approach for underwater sensor networks to assist a diver in distress, Sensors 21 (4) (2021) 1306.

[39] S. Sun, T. Liu, Y. Wang, G. Zhang, K. Liu, Y. Wang, High-rate underwater acoustic localization based on the decision tree, IEEE Trans. Geosci. Remote Sens. 60 (2021) 1–12.

[40] G. Allegro, A. Fascista, A. Coluccia, Acoustic dual-function communication and echo-location in inaudible band, Sensors 22 (3) (2022) 1284.

[41] B. Xu, S Li, A.A. Razzaqi, Y. Guo, L. Wang, A novel measurement information anomaly detection method for cooperative localization, IEEE Trans. Instrum. Meas. 70 (2021) 1–18.

[42] G. Han, A. Gong, H. Wang, M. Martínez-García, Y. Peng, Multi-AUV collaborative data collection algorithm based on Q-learning in underwater acoustic sensor networks, IEEE Trans. Veh. Technol. 70 (9) (2021) 9294–9305.

[43] H. Lohrasbi, T.A. Gulliver, Unknown RSSD-based localization CRLB analysis with semidefinite programming, IEEE Trans. Commun. 67 (5) (2019) 3791–3805.

[44] S. Song, J. Liu, J. Guo, C. Zhang, T. Yang, J. Cui, Efficient velocity estimation and location prediction in underwater acoustic sensor networks, IEEE Internet Things J. 9 (4) (2021) 2984–2998.

[45] B. Zhang, J. Zhu, Y. Wu, W. Zhang, M. Zhu, Underwater localization using differential doppler scale and TDOA measurements with clock imperfection, Wirel. Commun. Mob. Comput. (2022).

[46] M. Zhao, M. Yan, T. Li, Vision-based positioning: related technologies applications and research challenges, in: Proceedings of the IEEE 9th International Conference on Software Engineering and Service Science (ICSESS), 2018, pp. 531–535.

[47] M. Simka, P. Ladislav, On the RSSI-based indoor localization employing LoRa in the 2.4GHz ISM band, Radioengineering 31 (1) (2022) 135–143.

[48] F.R. Andersen, B. Kalpit Dilip, P. Martin Nordal, R. Sarah, Ranging capabilities of LoRa 2.4GHz, in: Proceedings of the *2020 IEEE 6th World Forum On Internet of Things (WF-IoT)*, IEEE, 2020, pp. 1–5.

[49] S.P. Robinson , P.A. Lepper and R.A. Hazelwood , 2014. Good practice guide for underwater noise measurement.

Azadeh Pourkabirian received the M.Sc. degree in Computer Network from Qazvin Azad University, Iran, in 2007, and the Ph.D. degree in Computer Science from Science and Research Branch of Azad University, Iran, in 2018. She is currently an Associate Professor with the Department of Computer Science and Information Technology, Qazvin Azad University. Her research interests include wireless communication, 5G, resource allocation, optimization, stochastic modeling, and game theory.

Fereshteh Kooshki received PhD degree with a thesis addressed optimizing the performance of multi-stage decision making systems in 2014. She has taught at the Azad University since 2008. Her research interests are optimization, modeling, performance analysis, benchmarking and decision science.

Mohammad Hossein Anisi is currently an Associate Professor with the School of Computer Science and Electronic Engineering, University of Essex, U.K. and Head of Internet of Everything (IoE) Laboratory. Prior to that, he worked as a Senior Researcher with the University of East Anglia, U.K. and Senior Lecturer with the University of Malaya, Malaysia, where he received the Excellent Service Award for his achievements. His research interests include IoT, WSN, Green and Energy-efficient Communication and Vehicular Networks. He has published more than 100 articles in high-quality journals and received several international and national funding awards for his fundamental and practical research as PI and Co-I. Dr Anisi is currently an associate editor of IEEE Transactions on Cybernetics, IEEE Transactions on Intelligent Transportation Systems, IEEE Transactions on Automation Science and Engineering and IEEE Transactions on AgriFood Electronics. Moreover, he has been lead organizer of special sessions and workshops at several IEEE conferences such as ICC, CAMAD, PIMRC, and VTC.

Anish Jindal is working as an Assistant Professor in Computer Science at Durham University, UK and is a visiting fellow in the School of Computer Science and Electronic Engineering (CSEE), University of Essex, UK. Prior to this, he worked as a Lecturer in CSEE, University of Essex and Senior Research Associate at the School of Computing Communications, Lancaster University, UK. He is the recipient of the Outstanding Ph. D. Dissertation Award, 2019 from the IEEE Technical Committee on Scalable Computing (TCSC) and conferred with the IEEE Communication Society's Outstanding Young Researcher Award for Europe, Middle East, and Africa (EMEA) Region, 2019. He has also been a visiting researcher to OFFIS - Institute for Information Technology, Germany in 2019. He is also the guest editor of various journals including Software: Practice and Experience (Wiley), Neural Computing Applications (Springer), Computer Communications (Elsevier), and IET Smart Cities (IET). His research interests are in the areas of smart cities, data analytics, artificial intelligence, cyber- physical systems, wireless networks, and security.